frontiers | Frontiers in Soft Matter

TYPE Original Research
PUBLISHED 11 October 2022
DOI 10.3389/frsfm.2022.1021077

OPEN ACCESS

EDITED BY
Suk-Won Choi,
Kyung Hee University, South Korea

REVIEWED BY
Dae-Shik Seo,
Yonsei University, South Korea
Kwang-Un Jeong,
Jeonbuk National University, South Korea

*CORRESPONDENCE
Deng-Ke Yang,
dyang@kent.edu

SPECIALTY SECTION
This article was submitted to Liquid Crystals,
a section of the journal
Frontiers in Soft Matter

RECEIVED 17 August 2022
ACCEPTED 21 September 2022
PUBLISHED 11 October 2022

CITATION
Halder S, Shin Y, Zhou Z, Zhang X, Hu L and Yang D-K (2022), Liquid crystal-polymer composites switchable windows for radiant energy flow and privacy control.
Front. Soft. Matter 2:1021077.
doi: 10.3389/frsfm.2022.1021077

Liquid crystal-polymer composites switchable windows for radiant energy flow and privacy control

Suman Halder[1], Yunho Shin[2], Ziyuan Zhou[2], Xinfang Zhang[2], Lang Hu[2] and Deng-Ke Yang[1,2]*

[1]Department of Physics, Kent State University, Kent, OH, United States, [2]Materials Science Program and Advanced Materials and Liquid Crystal Institute, Kent State University, Kent, OH, United States

Global warming is becoming a more and more severe crisis for humans. One way to resolve the concern is to reduce energy consumption. Smart switchable windows for office and residential buildings and vehicles can help reduce energy consumption. An ideal smart window should be able to control radiant energy flow and privacy. We investigated the capability of switchable windows based on liquid crystal/polymer composites, such as polymer dispersed liquid crystal (PDLC), polymer stabilized liquid crystal (PSLC), and polymer stabilized cholesteric texture (PSCT), to control the privacy and radiant energy flow. Through a systematic study, we identified methods to improve their capabilities. We demonstrated that PDLC and PSCT windows of sufficient thick film thickness can control both privacy and energy flow.

KEYWORDS

liquid crystal, liquid crystal/polymer composite, switchable windows, privacy control, radiant energy flow control

1 Introduction

Global warming, caused by fossil fuel energy consumption, imposes a big challenge on humans. Approximately 40% of the total energy is used to heat and cool office and residential buildings (Chel and Kaushik, 2018; Ke et al., 2018). Smart switchable windows can greatly help reduce this energy consumption (Lampert, 1998; Wong and Chan, 2014; Casini, 2015; Oh et al., 2019). An ideal window should have two functions. The first function is to control radiant energy flow (solar light). On a hot summer day, the window should prevent sunlight from flowing through the window and entering the building, thus keeping the building cool. While on a cold winter day, the window should let sunlight through to warm up the building. The second function is to control privacy. When no privacy is needed, the window is transparent in such a way that people inside the building can see outside sceneries. When privacy is needed, the window becomes opaque in such a way that people outside the building cannot see inside activities.

Liquid crystal/polymer composites have been used to make switchable windows (Castellón and Levy, 2018; Lee and Kumar, 2021). The three leading technologies are

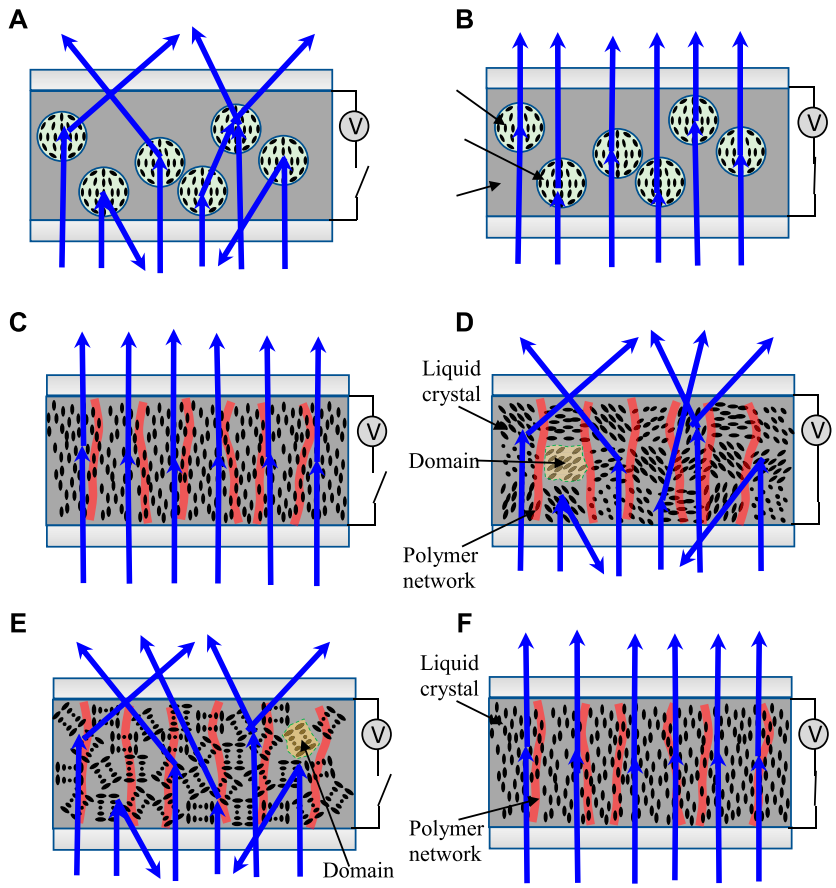

FIGURE 1
Schematic diagrams of liquid crystal/polymer composite switchable windows. **(A)** PDLC in voltage-off state, **(B)** PDLC in voltage-on state, **(C)** PSLC in voltage-off state, **(D)** PSLC in voltage-on state, **(E)** PSCT in voltage-off state, **(F)** PSCT in voltage-on state.

polymer dispersed liquid crystal (PDLC) switchable window, polymer stabilized liquid crystal (PSLC) switchable window, and polymer stabilized cholesteric texture (PSCT) switchable window (Bao et al., 2009; Khandelwal et al., 2015; Hemaida et al., 2020). They can be switched by voltages. In one voltage condition, the windows are transparent with high transmittance. In another voltage condition, they are optically scattering (Long and Ye, 2014; Fuh et al., 2017; Jiang et al., 2019).

PDLCs consist of an isotropic polymer and a nematic liquid crystal (Higgins, 2000; Bronnikov et al., 2013). The composite is sandwiched between two parallel substrates with a transparent electrode to produce the switchable window. There is no alignment layer on the surface of the substrates. The polymer concentration is high (~50%) and forms a binder. The liquid crystal forms micron-size droplets which are dispersed in the binder as shown in Figure 1A. The ordinary refractive index n_o of the liquid crystal is matched to the refractive index n_p of the polymer, while the extraordinary refractive index n_e of the liquid crystal is higher than n_p . The liquid crystal has a positive dielectric anisotropy and tends to align parallel to externally applied electric fields (Coates, 1995). In the absence of applied voltage, in different droplets, the liquid crystal orients in different directions randomly, as shown in Figure 1A. For a light incident normally to the PDLC film, it encounters different refractive indices in the polymer and liquid crystal, respectively, and thus is scattered (Li et al., 2008a; Pascault and Williams, 2009). When a sufficiently high voltage is applied, the liquid crystal is uniformly aligned along the film's normal direction, as shown in Figure 1B. The light encounters the same refractive index in the liquid crystal and polymer and thus is transmitted.

PSLCs consist of a polymer and a nematic liquid crystal (Kumar et al., 2011). The composite is sandwiched between two parallel substrates with a transparent electrode. There is a homeotropic alignment layer on the inner surface of the substrates. The polymer concentration is low (<10%). It forms an anisotropic polymer network in the normal direction of the film, as shown in Figure 1C. The liquid crystal has a negative dielectric anisotropy and tends to align perpendicular to

externally applied electric fields (Luckhurst and Dunmur, 2017). When no voltage is applied, both the liquid crystal and polymer network are aligned in the normal direction of the film, as shown in Figure 1C. For an incident light (in any direction) it encounters a uniform refractive index throughout the film and thus is transmitted (Yu et al., 2017). When a sufficiently high voltage is applied, the polymer network remains in the original direction while the liquid crystal is switched into a poly-domain structure, wherein different domains, the liquid crystal orients randomly in different directions (Zhou et al., 2020), as shown in Figure 1D. The incident light encounters different refractive indices in different domains and thus is scattered.

PSCTs consist of a polymer and a cholesteric liquid crystal (Crawford and Zumer, 1996; Yang, 2012). The cholesteric liquid crystal possesses a periodic helical structure. The periodicity, the distance along the helical axis over which the liquid crystal molecule rotates 360°, is known as the pitch. The composite is sandwiched between two parallel substrates with a transparent electrode. There is no alignment layer on the inner surface of the substrates. The polymer concentration is low (<10%). It forms an anisotropic polymer network in the normal direction of the film, as shown in Figure 1E. The liquid crystal has a positive dielectric anisotropy and tends to align parallel to the externally applied electric field. When no voltage is applied, the polymer network is uniformly aligned along the film's normal direction, while the liquid crystal is in a poly-domain state, called focal conic texture (or focal conic state) (Bao et al., 2009; Lee et al., 2015), as shown in Figure 1E. The helical axis of the liquid crystal varies from domain to domain, and thus the orientation of the liquid crystal varies from domain to domain. For an incident light (in any direction), it encounters different refractive indices from domain to domain and thus is scattered (Yang, 2012). When a voltage is applied, the helical axis is tilted toward the direction parallel to the cell substrate and the pitch is increased. When a sufficiently high voltage is applied, the helical structure is unwound (the pitch becomes infinitely long), and the liquid crystal is uniformly aligned along the film's normal direction, as shown in Figure 1F. The incident light encounters a uniform refractive index throughout the film and thus is transmitted (Yang, 2012).

All these three switchable windows are excellent for privacy control (Körner et al., 1994; Sanchez-Pena et al., 2002; Liang et al., 2011; Ji et al., 2017). They do not use polarizers and have very high transmittances (~90%) in the transparent state (Hurley et al., 2009; Ying-GueyFuh et al., 2009; Lin et al., 2011). The light loss is mainly caused by the reflection from the air-substrate interfaces. When they are in the scattering state, their scattering is strong, and images of sceneries seen through the windows are severely distorted by the scattering and cannot be distinguished. Their capability to control radiant energy flow control, however, is usually not the best and needs improvement. When the windows are in the scattering state, most of the incident light is scattered in forward directions and thus goes through the windows. Only about 20% of light is scattered in backward directions.

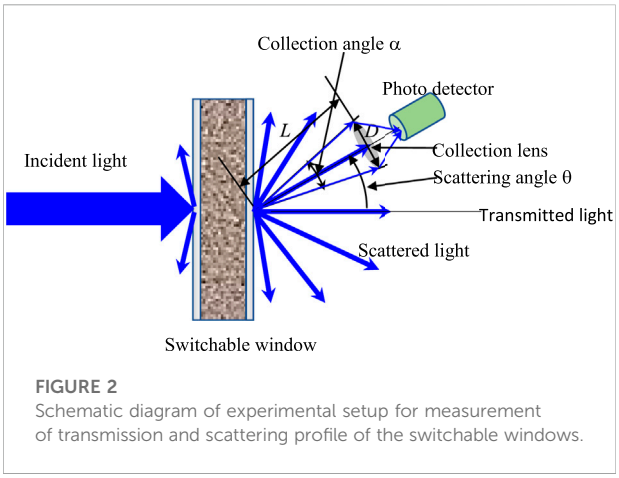

FIGURE 2
Schematic diagram of experimental setup for measurement of transmission and scattering profile of the switchable windows.

In this paper, we report our study of the scattering profiles of the three switchable windows and their capabilities of privacy and energy flow control. We also explored ways to improve their capability of energy flow control. Finally, we compare the performances of the three switchable windows.

2 Measurement of scattered light

The liquid crystal/polymer composite switchable windows are operated between a transparent state and a scattering state. When the incident light propagates through them, it is scattered in all directions, as shown in Figure 2. In our measurement, a green He-Ne laser light with the wavelength 543 nm was used, and the light is collimated and incident on the window in the normal direction. The incident light intensity is I_o. The intensity of the scattered light per unit solid angle is the scattered light intensity profile and is described by $i(\theta)$, where θ is the scattering (polar) angle. For the switchable windows discussed in this paper, the scattered light intensity depends only on the polar scattering angle, not the scattering azimuthal angle φ (not shown in Figure 2). The scattered light is collected by a convex lens which focuses the scattered light on the photo detector. The scattered light intensity detected by the detector depends on the solid angle of the collection lens. The distance between the incident point on the window and the lens is. The diameter of the lens is D. When $L \gg D$, the solid angle of the detector is given by

$$\Omega = 4\pi\left[\pi(D/2)^2/(4\pi)L^2\right] = (\pi/4)(D/L)^2 \quad (1)$$

Usually, the linear collection angle, defined by

$$\alpha = 2\arctan\left[(D/2)/L\right] \approx D/L \quad (2)$$

is used to specify the capability of the lens to collect scattered light. From Eqs. 1, 2, we have $\Omega = \pi\alpha^2/4$. The percentage of light scattered in the forward direction is given by

$$T_{FW} = \frac{\int_0^{\pi/2}\int_0^{2\pi} i(\theta)\sin\theta d\theta d\varnothing}{I_o} = \frac{2\pi\int_0^{\pi/2} i(\theta)\sin\theta d\theta}{I_o} \quad (3)$$

The percentage of light scattered in the backward direction is given by

$$T_{BW} = \frac{\int_{\pi/2}^{\pi}\int_0^{2\pi} i(\theta)\sin\theta d\theta d\Phi}{I_o} = \frac{2\pi\int_{\pi/2}^{\pi} i(\theta)\sin\theta d\theta}{I_o} \quad (4)$$

Usually, the collection angle α is less than 10°, and the scattered light intensity does not change much in the scattering angle region from $\theta - \alpha/2$ to $\theta + \alpha/2$, the total light intensity detected by the detector is given by

$$I(\theta) = i(\theta)\Omega = i(\theta)\pi\alpha^2/4 \quad (5)$$

In the transmittance measurement, the lens and the detector are placed at the polar angle of 0. Therefore, the transmittance is given by

$$T = \frac{2\pi\int_0^{\alpha/2} i(\theta)\sin\theta d\theta}{I_o} \approx \frac{2\pi\int_0^{\alpha/2} i(\theta=0)\sin\theta d\theta}{I_o} = \frac{2\pi i(\theta=0)[1-\cos(\alpha/2)]}{I_o} \approx \frac{i(\theta=0)\pi\alpha^2}{4I_o} \quad (6)$$

In measuring the capability of the switchable windows to control privacy, the collection angle of 4° is used. If the measured transmittance of the scattering state is less than 1%, good privacy control is achieved. In measuring the capability of the windows to control energy flow, the collection of 180° would be the best. This large collection angle can only be obtained with an integrating sphere. Unfortunately, we do not have an integrating sphere. As a compromise, we use the collection angle of 20°, which turns out to be able to give a good idea of the capability of the windows to control energy flow. In order to determine the capability more accurately, we measure the scattered light intensity profile and then use Eqs. 3, 4 to calculate the percentage of light scattered in the forward and backward directions.

3 Switchable window cell preparation

In preparing the cell for the switchable windows, the empty cell was first assembled. It consisted of two 1 mm thick parallel glass plates with ITO (indium tin oxide) coating which serves as the transparent electrode. The ITO coating was on the inner surface of the substrates. The cell thickness was controlled by spherical spacers. Secondly, the liquid crystal and monomer were mixed homogeneously. The mixture was filled into the cell by capillary action. Last, the cell was irradiated by a LED UV light with a wavelength of 365 nm at room temperature to polymerize the monomer.

In the fabrication of the PDLC switchable window, the liquid crystal used was E7 (from Merck), whose dielectric anisotropy $\Delta\varepsilon$ is +13.8 and birefringence Δn is 0.224. The isotropic monomer (prepolymer) used was NOA65 (from Norland Optical Adhesive Inc.). The concentration of E7 was 50%, and the concentration of NOA65 was also 50%. There was no alignment layer on the inner surface of the substrate.

In the fabrication of the PSLC switchable window, the liquid crystal used was BHR82 (from BaYi), whose dielectric anisotropy $\Delta\varepsilon$ is -7.6 and birefringence Δn is 0.237. The mesogenic monomer used was RM257 (from Merck). A small amount of photo-initiator benzoin methyl ether (BME) (from Polyscience) was added. The ratio between the concentrations of RM257 and BME was about 10: 1. There was a homeotropic alignment layer obtained by coating polyimide SE5661 (from Nissan Chemical) on the inner surface of the ITO substrates. The alignment layer was prebaked at 80°C for 5 min, followed by hard baking at 180°C for 1 h. The mixture of the liquid crystal, monomer, and photo-initiator was filled into the cell by capillary action. The cell was irradiated by UV light to polymerize the monomer.

In the fabrication of the PSCT switchable window, the mesogenic monomer used was RM257. A small amount of photo-initiator benzoin methyl ether (BME) (from Polyscience) was added. The ratio between the concentrations of RM257 and BME was about 10:1. The cholesteric liquid crystal used was constructed by mixing nematic liquid crystal E7 and chiral dopant R1011 (from Merck). The pitch P, an important parameter affecting the performance of the switchable window, of the cholesteric liquid crystal was controlled by the chiral dopant concentration according to the equation $P = 1/(HTP \cdot x)$, where HTP and x are the helical twisting power and concentration of the chiral dopant, respectively. The HTP of R1011 is about $30\mu m^{-1}$. There was no alignment layer on the inner surface of the substrates. The mixture of the liquid crystal, monomer, and photo-initiator was filled into the cell by capillary action. The cell was irradiated by UV light to polymerize the monomer. During the irradiation, a sufficiently high 1 kHz AC voltage was applied such that the liquid crystal was in the homeotropic state, where the helical structure of the liquid crystal was unwound, and the liquid crystal was unidirectionally aligned in the cell's normal direction.

4 Electro-optical properties

4.1 Polymer dispersed liquid crystal switchable window

The scattering of the PDLC depends on the birefringence of the liquid crystal, liquid crystal droplet size, and cell

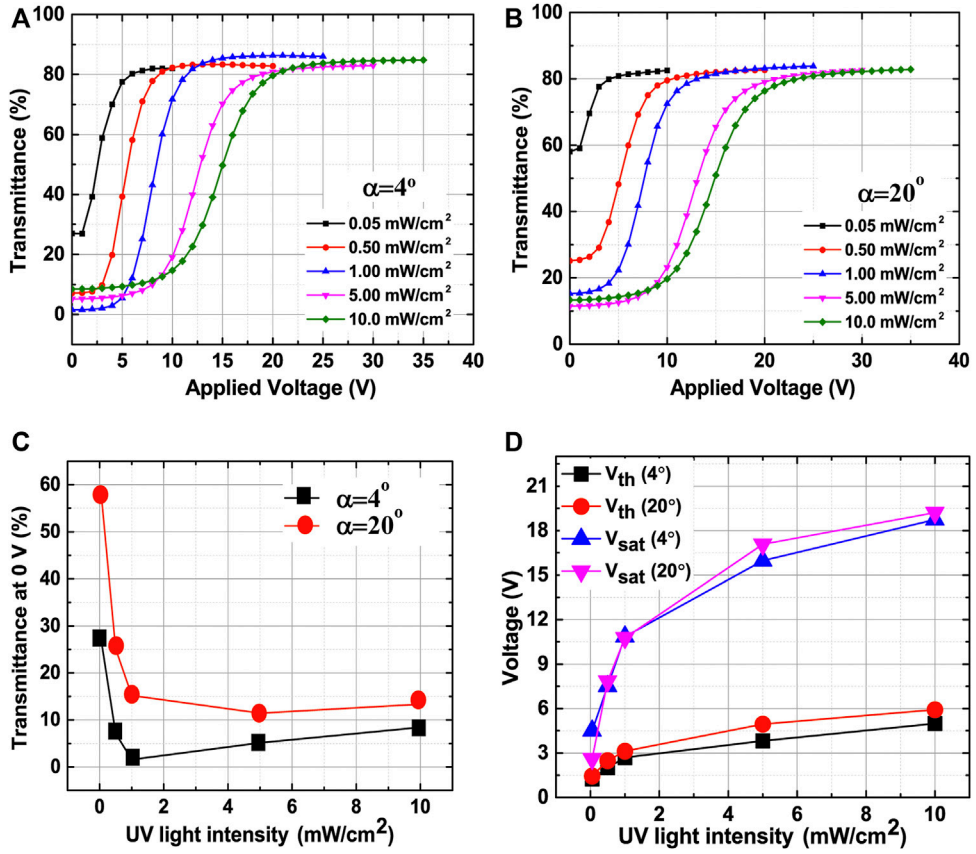

FIGURE 3
Electro-optical properties of the PDLC windows with the cell thickness of 10 μm cured under various UV light intensity. **(A)** Transmittance vs applied voltage measured with the collection angle of 4°. **(B)** Transmittance vs applied voltage measured with the collection angle of 20°. **(C)** Transmittance of scattering state vs curing UV light intensity. **(D)** Threshold and saturation voltages vs curing UV light intensity.

thickness. The birefringence depends on the molecular structure of the liquid crystal. Liquid crystals with large birefringence exhibit strong scattering and are desirable for switchable windows. In our experiment, only one liquid crystal is used; thus, the effect of birefringence is not studied. Our research is focused on studying the effects of liquid crystal droplet size and cell thickness.

First, we studied the effects of liquid crystal droplet size on the electro-optical properties of the PDLC window. The cell thickness is kept at 10 μm. We vary the droplet size by using different curing UV light intensities. Under a high UV light intensity, the polymerization speed of the monomer is faster, and thus smaller droplets form (Lackner et al., 1989; Li et al., 2008b). When the collection angle is 4°, the transmittance as a function of the applied voltage is shown in Figure 3A. When the curing UV light intensity is 0.05 mW/cm^2, the transmittance T_{min} of the scattering state (at 0 V) is 27.0% because the droplet size is too large (much larger than the wavelength of the incident light), and the material is not very scattering (Drzaic, 1995; Paul Montgomery et al., 1998; Kelly et al., 2006). When the applied voltage is increased above 5 V, the liquid crystal droplets are gradually aligned in the cell's normal direction, and thus the transmittance increases. When the applied voltage is increased to 20 V, the maximum (saturated) transmittance of 82% is reached. As the UV light intensity is increased, the droplet size decreases. When the UV light intensity is increased from 0.05 mW/cm^2 to 1.0 mW/cm^2, the transmittance of the scattering state decreases dramatically to 1.6%, as shown in Figure 3C. When the UV light intensity is increased further, the transmittance of the scattering state increases slightly. When the UV light intensity is increased, the driving voltage increases because it becomes more difficult to align the liquid crystal in the cell's normal direction in smaller droplets (Nastal Ł et al., 1999; Seo et al., 2014). The maximum transmittance T_{max}, namely the transmittance of the transparent state, is about 82%, approximately independent of the UV light intensity. The light loss is caused by the reflection from the glass-air interfaces and glass-ITO interfaces and the residual scattering of the material due to the imperfect alignment of the liquid crystal. We use two voltages to characterize the driving voltage. One is the threshold voltage V_{th}, the voltage at which the

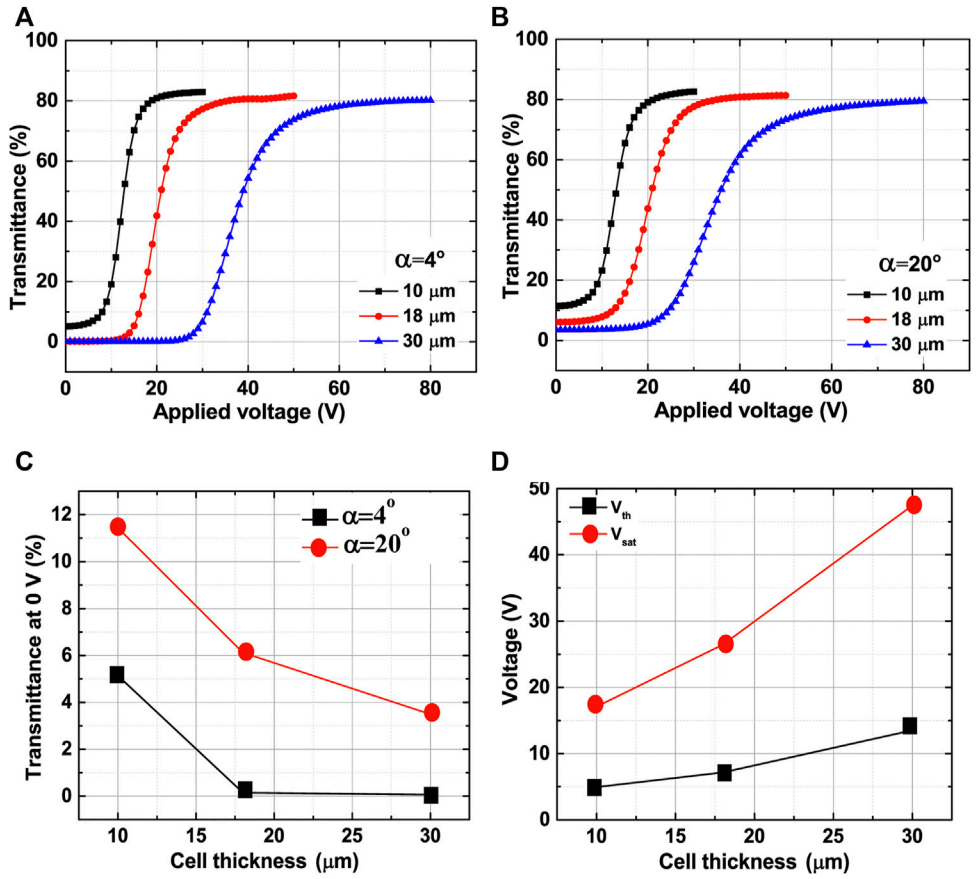

FIGURE 4
Electro-optical properties of the PDLC windows with different cell thicknesses cured under a UV light intensity of 5 mW/cm^2. **(A)** Transmittance vs applied voltage measured with the collection angle of 4°. **(B)** Transmittance vs applied voltage measured with the collection angle of 20°. **(C)** Transmittance of scattering state vs cell thickness. **(D)** Threshold and saturation voltages vs cell thickness.

transmittance becomes $T_{min} + 0.1\,(T_{max} - T_{min})$. The other one is the saturation voltage V_{sat}, the voltage at which the transmittance becomes $T_{min} + 0.9\,(T_{max} - T_{min})$. When the UV light intensity is increased, both the threshold and saturation voltage increase, as shown in Figure 3D. When the collection angle is 20°, the transmittance as a function of the applied voltage is shown in Figure 3B. The transmittance of the scattering state is much higher because more scattered light in forward directions is detected. The transmittance of the scattering state as a function of the curing UV light intensity is shown in Figure 3C. When the curing UV light intensity is 0.05 mW/cm^2, the transmittance T_{min} of the scattering state (at 0 V) is 58.0%. When the UV light intensity is increased, the transmittance of the scattering state decreases. The minimum scattering state transmittance of 11.1% is obtained when the UV light intensity is 5 mW/cm^2, different from that when the collection angle is 4°, where the minimum scattering state transmittance is obtained when the UV light intensity is 1 mW/cm^2. This difference indicates that the scattering light intensity profile depends on the droplet size. For big droplets, light is mainly scattered in directions with small scattering angles. For small droplets, light is more scattered in directions with large scattering angles. Therefore, in order to increase the capability of the window to control energy flow, the droplet size should be small. A qualitative argument for the different scattered light intensity profiles of PDLCs with different droplet sizes can be made in the following way. The scattering strength at a given scattering wavevector is proportional to the square of the amplitude of the Fourier component of the dielectric constant at that wavevector. When the droplet size is small, the amplitude of the Fourier components of the refractive index of the material is peaked at a large wavevector. The scattering wavevector increases with the scattering angle for an incident light with a fixed wavelength. Therefore, a PDLC with small droplets can better control energy flow. The driving voltage is almost independent of the collection angle, as shown in Figure 3D. In future discussions, we do not show the driving voltage measured with the collection angle of 20°.

We then studied the effects of cell thickness on the electro-optical properties of the PDLC window. The curing UV light intensity is fixed at 5 mW/cm^2, and thus the liquid crystal droplet size is fixed. We vary the cell thickness (PDLC film thickness). When the collection angle is 4°, the transmittance as a function of the applied voltage is shown in Figure 4A. When the cell thickness is 10 μm, the transmittance T_{min} of the scattering state (at 0 V) is 5.15%. When the cell thickness is increased to 18 μm, the transmittance of the scattering state decreases dramatically to 0.15%, as shown in Figure 4C. When the cell thickness is increased to 30 μm, the transmittance of the scattering state decreases to 0.06%. When the cell thickness is increased, the driving voltage increases approximately linearly, as shown in Figure 4D. The electric field needed to switch the PDLC window depends only on the droplet size. The driving voltage equals the product of the required electric field and cell thickness. When the droplet size is fixed, the needed electric field is fixed, and the driving voltage increases linearly with the cell thickness.

Linearly with the cell thickness. The maximum transmittance T_{max} , namely the transmittance of the transparent state, decreases slightly with the cell thickness because of the residual scattering of the transparent state due to the imperfect match of the refractive indices of the liquid crystal and polymer. When the collection angle is 20°, the transmittance as a function of the applied voltage is shown in Figure 4B. The transmittance of the scattering state is higher with the larger collection angle, because more scattered light in forward directions is detected. The transmittance of the scattering state as a function of the cell thickness is shown in Figure 4C. When the cell thickness is 10 μm, the transmittance T_{min} of the scattering state (at 0 V) is 11.1%. When the cell thickness is 18 μm, the transmittance of the scattering state (at 0 V) is 6.1%. When the cell thickness is 30 μm, the transmittance of the scattering state (at 0 V) is 3.5%. Interestingly, the trend of the dependence of the scattering state transmittance on cell thickness depends on the collection angle. This phenomenon is probably caused by the transition from single scattering regime to multiple scattering regime when the cell thickness increases. In the single scattering regime, the transmittance decreases dramatically with cell thickness as a negative exponential function. In the multiple scattering regime, the transmittance decreases slowly with cell thickness as a negative linear function (Marinov et al., 2009). When the cell thickness is 10 μm or 18 μm, the scattering of the PDLC is in the single scattering regime. When the cell thickness is 30 μm, the scattering of the PDLC is in the multiple scattering regime. Furthermore, the scattered light intensity profile depends on whether the scattering is the single or multiple scattering regime. In the single scattering region, light is mainly scattered in directions with small scattering angles, while in the multiple scattering region, more light is scattered in directions with large scattering angles (Klosowicz and Zmija, 1995). For the collection angle of 4°, when the cell thickness is increased from 10 μm to 18 μm and then 30 μm, the transmittance decreases by a factor of 34 first and then a factor of 2.5. For the collection angle of 20°, when the cell thickness is increased from 10 μm to 18 μm and then 30 μm, the transmittance decreases by a factor of 1.8 first and then a factor of 1.7.

4.2 Polymer stabilized liquid crystal switchable window

The scattering of the PSLC depends on the birefringence of the liquid crystal, liquid crystal domain size, and cell thickness. Since we only used one liquid crystal in our experiment, the birefringence effect was not studied. Therefore, our research is focused on exploring the effects of liquid crystal domain size and cell thickness.

In PSLCs, the liquid crystal domain size can be adjusted by the monomer concentration and the curing UV light intensity (Rajaram et al., 1996; Dierking et al., 1998a). We first studied the effect of monomer concentration. The cell thickness is kept at 10 μm, and the curing UV light intensity is fixed at 5 mW/cm^2. The monomer concentration is varied. When the collection angle is 4°, the transmittance as a function of the applied voltage is shown in Figure 5A. For the window with 3% monomer, when no voltage is applied, the material is in the transparent state with the transmittance of about 90%, where there is almost no residual scattering. When the applied voltage is increased above 5 V, the liquid crystal is tilted away from the cell's normal direction, liquid crystal domains start forming, and the transmittance decreases. When the applied voltage is increased to 23 V, the transmittance decreases to a minimum value T_{min} of 4.1%. As the monomer concentration is increased, the transmittance of the transparent state does not change, but the transmittance of the scattering state (when sufficiently high voltage is applied) first decreases, as shown in Figure 5C, indicating the liquid crystal domain size is decreased. When the monomer concentration is 4%, 5%, 6% and 7%, respectively, the corresponding transmittance of the scattering state is 0.72%, 0.65%, 0.32% and 0.17%. When the monomer concentration is increased further, the transmittance of the scattering state increases slightly. When the monomer concentration is 8% and 10%, respectively, the corresponding transmittance of the scattering state is 0.52%, and 0.77%. Therefore, the capability of the PSLC windows to control privacy is good when the monomer concentration is equal to and higher than 4%. The change of the transmittance of the scattering state is caused by the change of the liquid crystal domain size. When the monomers are polymerized, they form an anisotropic polymer network (Broer et al., 1990; Fung et al., 2006; Yang, 2012). The space between the fibrils of the polymer network is occupied by the liquid crystal. When the monomer concentration is increased, the density of the formed polymer fibril increases, and the distance between neighboring fibrils decreases; therefore, the liquid crystal domain size decreases. When the domain size is about twice of the wavelength of visible

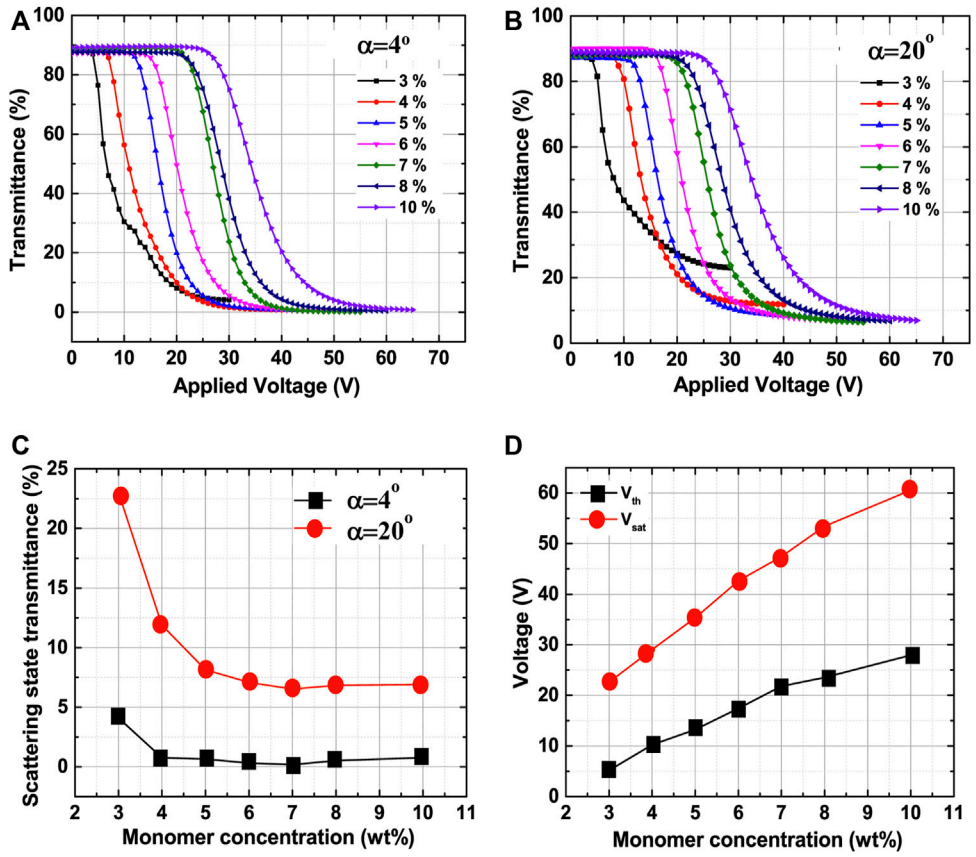

FIGURE 5
Electro-optical properties of the PSLC windows with different monomer concentrations cured under a UV light intensity of 5 mW/cm^2. **(A)** Transmittance vs applied voltage measured with the collection angle of 4°. **(B)** Transmittance vs applied voltage measured with the collection angle of 20°. **(C)** Transmittance of scattering state vs monomer concentration. **(D)** Threshold and saturation voltages vs monomer concentration.

light, the material is most scattering. The driving voltages increase approximately with the monomer concentration, as shown in Figure 5D. The formed polymer network has an aligning effect on the liquid crystal, which is linearly proportional to the monomer concentration, and tends to keep the liquid crystal in the cell's normal direction (Ma and Yang, 2000; Yang, 2012; Yang et al., 2013; Halder et al., 2021). The applied voltage must overcome the aligning effect of the polymer network in order to switch the liquid crystal to the poly-domain scattering state. When the collection angle is 20°, the transmittance as a function of the applied voltage is shown in Figure 5B. When no voltage is applied, the material is in the transparent state with the transmittance of about 90%, the same as when the collection angle of 4° is used. When the applied voltage is increased, the transmittance decreases. When the monomer concentration is 3%, the transmittance of the scattering state is 23.0%. When the monomer concentration is increased to 4%, the transmittance of the scattering state decreases to 11.9%. When the monomer concentration is decreased further, the transmittance of the scattering state does not change much and remains around 7%, as shown in Figure 5C.

We then varied the liquid crystal domain size by using different UV light intensities. The monomer concentration is fixed at 6%, and the cell thickness is fixed at 10 μm. When the collection angle is 4°, the transmittance as a function of the applied voltage is shown in Figure 6A. The transmittance of the transparent state (at 0 V) is high, about 90%. When the applied voltage is increased, the transmittance decreases. When the UV light intensity is 0.05 mW/cm^2, the transmittance of the scattering state (at 25 V) is 3.02%. When the UV light intensity is increased to 0.5 mW/cm^2, the transmittance of the scattering state decreases to 0.79%, as shown in Figure 6C. When the UV light intensity is increased further, the transmittance of the scattering state decreases slightly. When the UV light intensity is 10 mW/cm^2, the transmittance of the scattering state is 0.21%. When the UV light intensity is increased, first, the driving voltages increase dramatically, and then only slightly, as shown in Figure 6D. The change of the transmittance of the scattering state and the driving voltage with the UV light

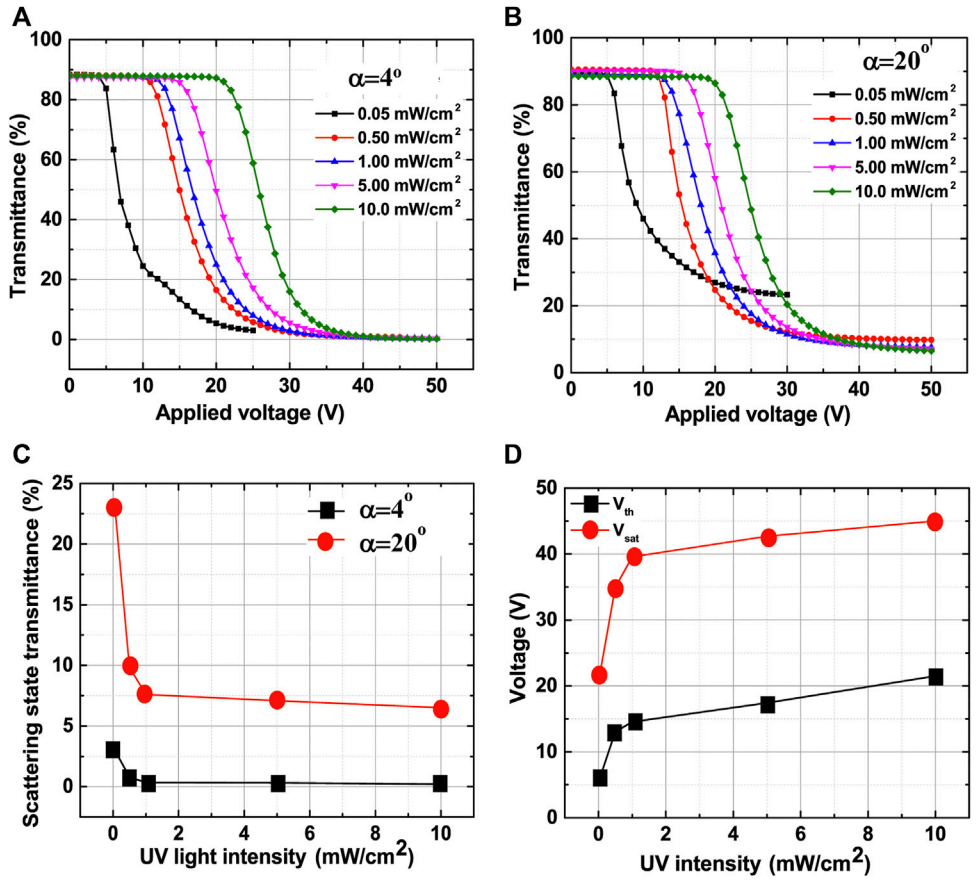

FIGURE 6
Electro-optical properties of the PSLC windows with 6% monomer cured under various UV light intensities. **(A)** Transmittance vs applied voltage measured with the collection angle of 4°. **(B)** Transmittance vs applied voltage measured with the collection angle of 20°. **(C)** Transmittance of scattering state vs curing UV light intensity. **(D)** Threshold and saturation voltages vs curing UV light intensity.

intensity indicates that when the UV light intensity is increased from 0.05 mW/cm^2 to 0.5 mW/cm^2, the liquid crystal domain size changes significantly, and beyond that, the domain size only changes slightly. When the collection angle is 20°, the transmittance as a function of the applied voltage is shown in Figure 6B. When no voltage is applied, the material is in the transparent state with the transmittance of about 90%, the same as when the collection angle of 4° is used. When the applied voltage is increased, the transmittance decreases. When the UV light intensity is 0.05 mW/cm^2, the transmittance of the scattering state is 23.0%. When the UV light intensity is increased to 0.5 mW/cm^2, the transmittance of the scattering state decreases to 9.8%. When the UV light intensity is further reduced, the transmittance of the scattering state does not change much and remains around 7%, as shown in Figure 6C.

We also studied the effects of cell thickness on the electro-optical properties of the PSLC window. The monomer concentration is fixed at 6%, and the curing UV light intensity is fixed at 5 mW/cm^2, and thus the liquid crystal domain size is fixed. The cell thickness is varied. When the collection angle is 4°, the transmittance as a function of the applied voltage is shown in Figure 7A. The transmittance of the transparent state (at 0 V) is near 90%, independent of the cell thickness. When the cell thickness is 10 μm, the transmittance T_{min} of the scattering state (at 45 V) is 0.32%. When the cell thickness is increased to 18 μm, the transmittance of the scattering state (at 80 V) decreases to 0.12%, as shown in Figure 7C. When the cell thickness is increased to 30 μm, the transmittance of the scattering state (at 110 V) decreases to 0.09%. When the cell thickness is increased, the driving voltage increases approximately linearly, as shown in Figure 7D. When the collection angle is 20°, the transmittance as a function of the applied voltage is shown in Figure 7B. The transmittance of the scattering state is higher because more scattered light in forward directions is detected. The transmittance of the scattering state as a function of the cell thickness is shown in Figure 7C. When the cell thickness is 10 μm, the transmittance T_{min} of the scattering state (at 45 V) is 7.1%. When the cell thickness is 18 μm, the

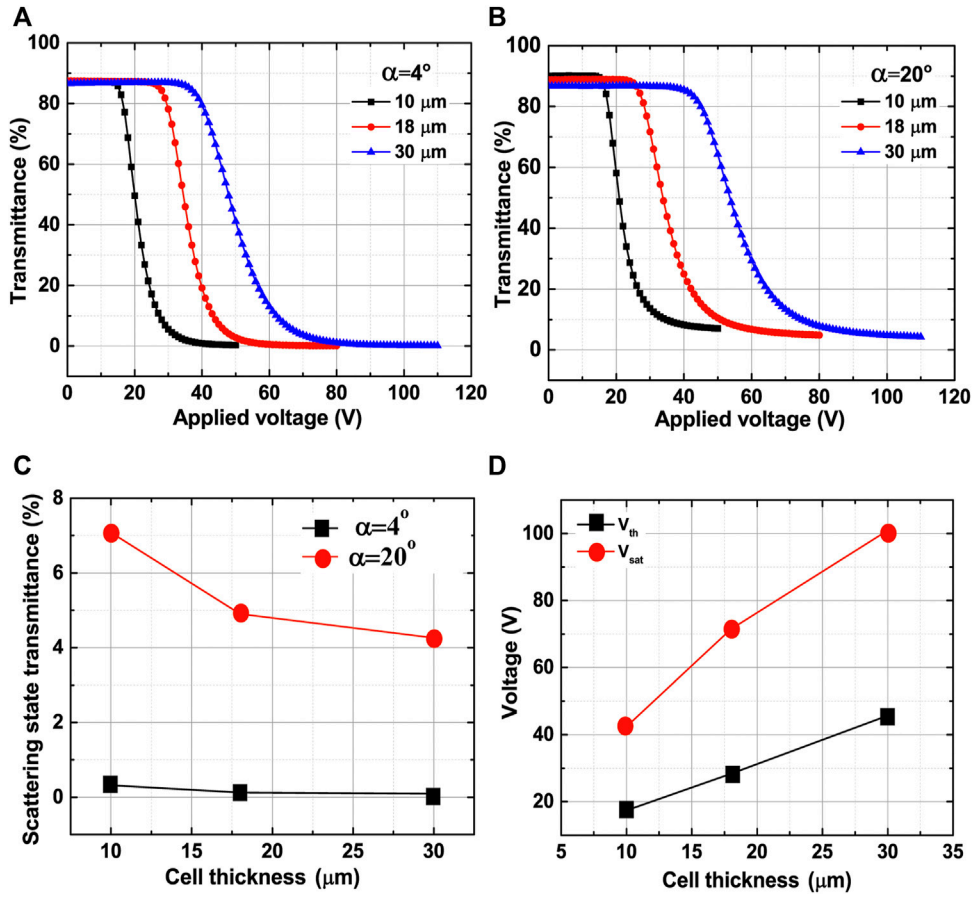

FIGURE 7
Electro-optical properties of the PSLC windows with different cell thicknesses cured under a UV light intensity of 5 mW/cm^2. **(A)** Transmittance vs applied voltage measured with the collection angle of 4°. **(B)** Transmittance vs applied voltage measured with the collection angle of 20°. **(C)** Transmittance of scattering state vs cell thickness. **(D)** Threshold and saturation voltages vs cell thickness.

transmittance of the scattering state (at 80 V) is 4.9%. When the cell thickness is 30 μm, the transmittance of the scattering state (at 110 V) is 4.3%. Therefore, it is not so efficient to increase the capability of controlling energy flow by increasing the cell thickness.

4.3 Polymer stabilized cholesteric texture switchable window

The scattering of a PSCT depends on the birefringence of the liquid crystal, liquid crystal domain size, and cell thickness. Like PDLCs and PSLCs, in this experiment, only one liquid crystal is used; thus, the effects of birefringence are not studied. Our research effort concentrates on studying the effects of liquid crystal domain size and cell thickness.

The electro-optical properties of PSCTs mainly depend on the monomer concentration and the helical pitch of the liquid crystal and slightly dependent on the curing UV light intensity (Dierking et al., 1998b; Huang et al., 2006; Xu et al., 2016). In our experiment, the curing UV light intensity is fixed at 5 mW/cm^2. We first studied the effect of monomer concentration. The pitch is fixed at 0.7 μm, and the cell thickness is 10 μm. The monomer concentration is varied. When the collection angle is 4°, the transmittance as a function of the applied voltage is shown in Figure 8A. For the window with 2.5% monomer, when no voltage is applied, the material is in the scattering state with the minimum transmittance T_{min} of 0.32%. When the applied voltage is increased to 21 V, the transmittance starts to increase. As the applied voltage is increased, the pitch increases and the domain size increases, and therefore the material becomes less scattering and the transmittance increases. When the applied voltage is increased above 28 V, the maximum transmittance T_{max} of 89% is reached. There is a large hysteresis in the transition between the scattering and transparent states. With decreasing voltage, the material

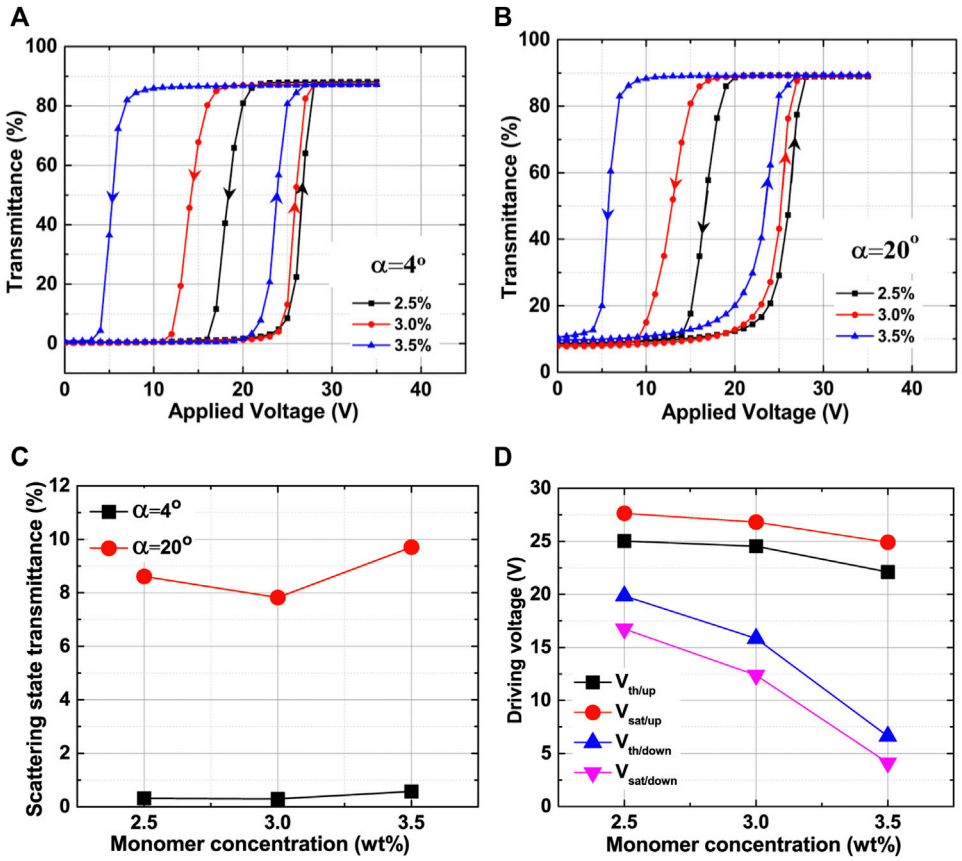

FIGURE 8
Electro-optical properties of the PSCT windows of the pitch of 0.7 μm with various monomer concentrations. **(A)** Transmittance vs applied voltage measured with the collection angle of 4°. **(B)** Transmittance vs applied voltage measured with the collection angle of 20°. **(C)** Transmittance of scattering state vs monomer concentration. **(D)** Threshold and saturation voltages vs monomer concentration.

remains in the transparent state until the voltage is decreased below 22 V. When the applied voltage is decreased further, the transmittance decreases. When the applied voltage is decreased to 0 V, the material transforms back to the scattering state with the minimum transmittance. When the monomer concentration is increased, the transmittance of the scattering state (at 0 V) does not change much, as shown in Figure 8C. When the monomer concentration is 3.0%, the transmittance of the scattering state is 0.29%. When the monomer concentration is 3.5%, the transmittance of the scattering state is 0.57%. The transmittance of the transparent state does not change with the monomer concentration, remaining around 89%. The driving voltage to switch the material from the scattering state to the transparent state decreases slightly with the monomer concentration. The hysteresis, defined as the difference between the voltage at which the transmittance is increased from T_{min} to $T_{min} + 0.5(T_{max} - T_{min})$ and the voltage the transmittance is decreased from T_{max} to $T_{min} + 0.5(T_{max} - T_{min})$, increases with the monomer concentration. The formed polymer network in the PSCT is anisotropic and aligned in the cell's normal direction. It has an aligning effect on the liquid crystal, which tends to rotate the liquid crystal to the transparent state. When the collection angle is 20°, the transmittance as a function of the applied voltage is shown in Figure 8B. When no voltage is applied to the sample with 2.5% monomer, the material is in the scattering state with a minimum transmittance T_{min} of 8.6%. When the monomer concentration is 3.0%, the transmittance of the scattering state is 7.8%. When the monomer concentration is 3.5%, the transmittance of the scattering state is 9.7%. This result indicates that the monomer concentration does not affect much the liquid crystal domain size.

We then studied the effects of the helical pitch of the cholesteric liquid crystal. In the experiment, the curing UV light intensity is fixed at 5 mW/cm^2. The monomer concentration is 3%, and the cell thickness is 10 μm. The transmittance of the scattering state (at 0 V) as a function of pitch is shown in Figure 9A. For both collection angles, when the pitch is increased from 0.5 μm to 0.7 μm, the transmittance of the

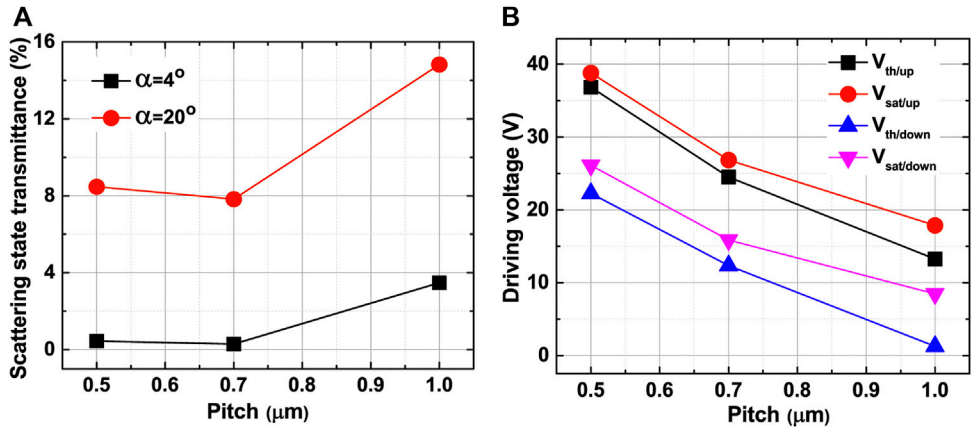

FIGURE 9
Electro-optical properties of the PSCT windows of monomer concentration of 3% with various the pitches. **(A)** Transmittance of scattering state vs pitch. **(B)** Threshold and saturation voltages vs pitch.

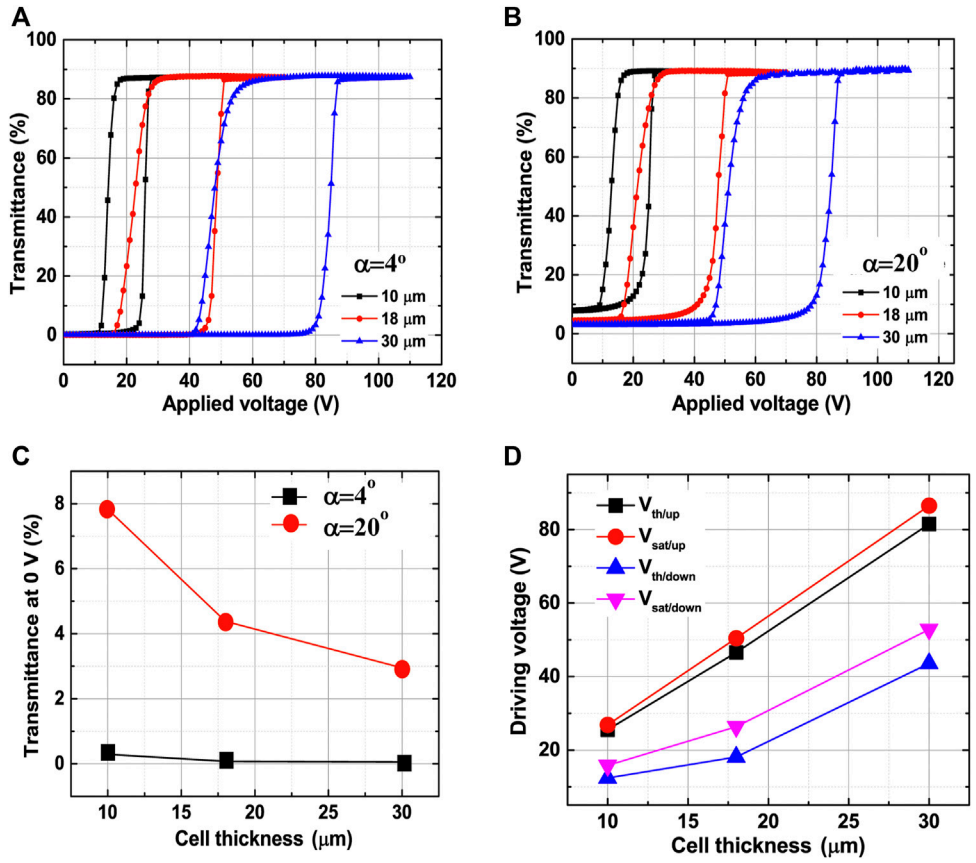

FIGURE 10
Electro-optical properties of the PSCT windows with the pitch of μm and monomer concentration of 3% of different cell thicknesses. **(A)** Transmittance vs applied voltage measured with the collection angle of 4°. **(B)** Transmittance vs applied voltage measured with the collection angle of 20°. **(C)** Transmittance of scattering state vs cell thickness. **(D)** Threshold and saturation voltages vs cell thickness.

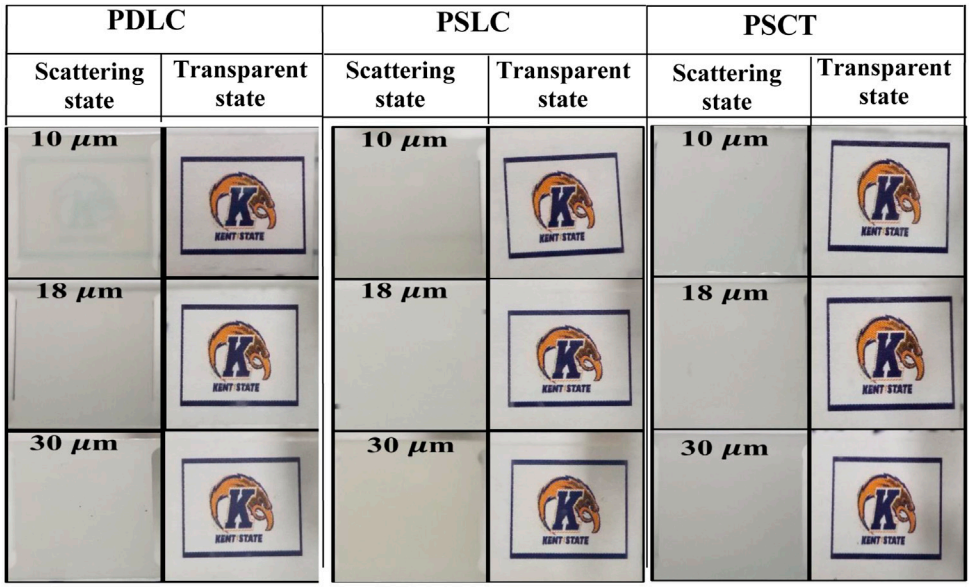

FIGURE 11
Photographs of the switchable windows in the scattering and transparent states of different cell thicknesses.

scattering state decreases slightly. When the pitch is increased further to 1.0 μm, the transmittance increases significantly. The pitch is a critical factor in determining the liquid crystal domain size. The domain size increases with the pitch (Huang et al., 2006). When the pitch is 1.0 μm, the domain size is too large, and the material does not strongly scatter visible light. The driving voltage as a function of the pitch is shown in Figure 9B. Both the threshold voltage and saturation voltages decrease monotonically with the pitch. In the transparent state, the helical structure is unwound, as shown in Figure 1F. The longer the pitch, the lower the required voltage to unwind the helical structure, following the equation $V = \pi^2 (h/P)\sqrt{K_{22}/\varepsilon_o \Delta\varepsilon}$, where K_{22} and $\Delta\varepsilon$ are the twist elastic constant and dielectric anisotropy, respectively. With the consideration of the transmittance of the scattering state and driving voltage, the best result is obtained with the pitch of 0.7 μm and monomer concentration of 3%.

We also studied the effect of cell thickness on the electro-optical properties of the PSCT window. The monomer concentration is fixed at 3%, the pitch is fixed at 0.7 μm, and the curing UV light intensity is fixed at 5 mW/cm^2, and thus the liquid crystal domain size is fixed. The cell thickness is varied. When the collection angle is 4°, the transmittance as a function of the applied voltage is shown in Figure 10A. When the cell thickness is 10 μm, the transmittance T_{min} of the scattering state (at 0 V) is 0.29%. When the cell thickness is increased to 18 μm, the transmittance of the scattering state decreases to 0.07%, as shown in Figure 10C. When the cell thickness is increased to 30 μm, the transmittance of the scattering state decreases to 0.05%. Note that the scattering of the 30 μm PSCT window is very strong, and the measured transmittance with the collection angle of 4° may not be accurate. When the cell thickness is increased, the driving voltage increases approximately linearly, as shown in Figure 10D. The transmittance of the transparent state (at sufficiently high voltage) remains around 89%, independent of the cell thickness. When the collection angle is 20°, the transmittance as a function of the applied voltage is shown in Figure 10B. The transmittance of the scattering state is higher because more scattered light in forward directions is detected. The transmittance of the scattering state as a function of the cell thickness is shown in Figure 10C. When the cell thickness is 10 μm, the transmittance T_{min} of the scattering state is 7.8%. When the cell thickness is 18 μm, the transmittance of the scattering state is 4.4%. When the cell thickness is 30 μm, the transmittance of the scattering state is 2.9%. The PSCT window has a better capability to control energy flow than the PDLC and PSLC windows.

5 Privacy control

We examined the capability of the switchable window to control privacy. In the experiment, a picture of the Kent State University logo is placed 1 cm behind the window. The appearance of the logo is visually observed and photographed. The photographs of the windows of various cell thicknesses are shown in Figure 11. For the PDLC windows, the curing UV light intensity is 5 mW/cm^2. For

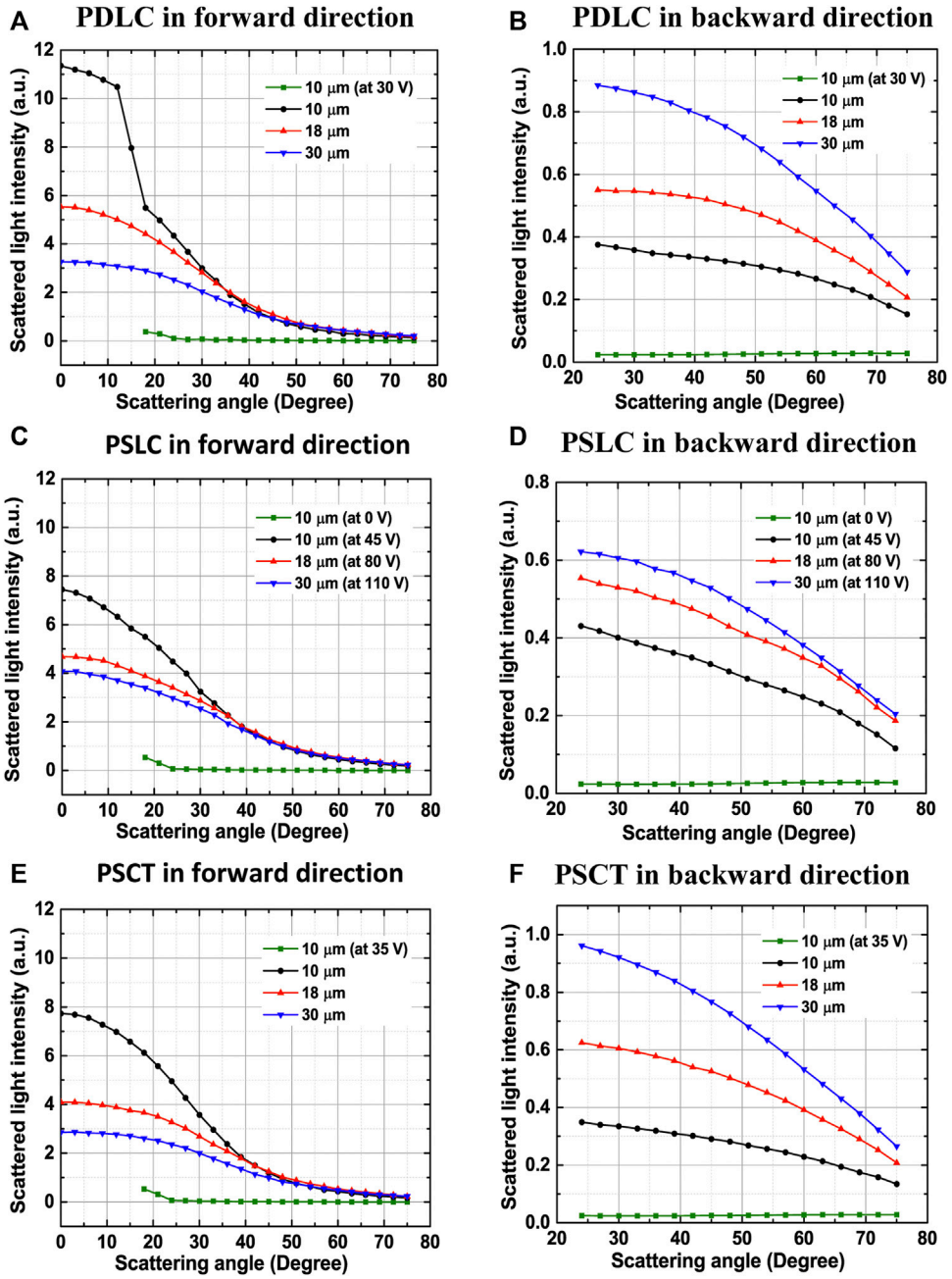

FIGURE 12
Scattered light intensity vs scattering angle of the windows with various cell thicknesses. **(A)** PDLC in forward directions, **(B)** PDLC in backward directions, **(C)** PSLC in forward directions, **(D)** PSLC in backward directions. **(E)** PSCT in forward directions, **(F)** PSCT in backward directions.

the PSLC windows, the monomer concentration is 6% and the curing UV light intensity is 5 mW/cm^2. For the PSCT windows, the monomer concentration is 3%, the pitch is 0.7 μm, and the curing UV light intensity is 5 mW/cm^2. For the PDLC window of the cell thickness of 10 μm, the logo can be seen when it is in the scattering state. It does not control privacy well. The PSLC window of the cell thickness of 10 μm is better. The logo can barely be seen when it is in the scattering state. The PSCT window of the cell thickness of 10 μm is the best; when it is in the scattering state, the logo cannot be seen. It controls privacy well. For the windows of cell thickness of 18 μm or 30 μm, when they are in the scattering state, the logo cannot be seen. They all have good capability of privacy control. The logo can be clearly

TABLE 1 Percentage of the light blocked by PDLC, PSLC, and PSCT switchable windows of different cell thicknesses and driving voltage.

Window type	Thickness (μm)	Percent of light blocked in scattering state (%)	Transmittance of transparent state (%)	Driving voltage (V)
PDLC	10	13	82	30
	18	27	81	50
	30	45	80	80
PSLC	10	14	88	50
	18	25	88	80
	30	33	87	110
PSCT	10	10	88	30
	18	29	88	50
	30	45	88	90

seen through on all the windows when they are in the transparent state.

6 Energy flow control

Although the transmittance of the windows measured with the collection angle of 20° gives an idea of their capability to control energy flow, a better measurement is needed to characterize their capability. In order to accomplish this task, we measured the scattered light intensity profile, namely the scattered light intensity as a function of the scattering angle of the switchable windows. In the measurement, the collection angle of 20° is used, which assures a high signal-to-noise ratio. In the forward direction, the scattered light intensity is measured in the scattering angle region from 0° to 75°. It is difficult to measure the scattered light intensity in the region from 75° to 90° because of the usage of the collection lens. In the backward direction, the scattered light intensity is measured in the scattering angle region from 25° to 75°. It is difficult to measure the scattered light intensity in the region from 75° to 90° because of the usage of the collection lens. It is also difficult to measure the scattered light intensity in the region from 0° to 25° where the detector would block the incident light. The PDLC windows studied are cured under the UV light intensity of 5 mW/cm^2. The PSLC windows studied have a monomer concentration of 6% and are cured under the UV light intensity of 5 mW/cm^2. The PSCT windows have the pitch of 0.7 μm and monomer concentration of 3% and are cured under the UV light intensity of 5 mW/cm^2. The results are shown in Figure 12. When the cell thickness is increased, the scattered light in forward directions with small scattering angle decreases significantly, while the scattered light in backward directions increases significantly. This is probably due to multiple scattering. When the cell is thin, single scattering is dominant, and most of the light is scattered in forward directions with small scattering angles. When the cell thickness is increased to 30 μm, multiple scattered becomes dominant. When light is scattered multiple times, a significant percentage of light is scattered in backward directions. For the same cell thickness, PSLC windows have the weakest backward scattering, PDLC windows have the medium backward scattering, and PSCT windows have the strongest backward scattering. This is probably attributed to the small liquid crystal domain size and the helical structure of the cholesteric liquid crystal in PSCT windows. Small domains produce more backward scattering. The periodic helical structure causes Bragg reflection. The wavelength of the reflected light is given by $\lambda = \bar{n}P\cos\gamma$, where $\bar{n}$ and P are the average refractive index and pitch of the liquid crystal, respectively, and γ is the incident angle of light with respect to the helical axis. For the cholesteric liquid crystal used in the PSCT windows, $\bar{n}\approx$ 1.6 and = 0.7. When the incident angle γ is 61°, the green laser light is reflected.

The switchable windows in the transparent state exhibit very weak scattering. More than 82% of incident light goes through the windows. The light blocked is mainly due to the reflection by the window substrate-air interfaces. The capability of the switchable windows to control energy flow depends on the percentage of light scattered in forward directions when they are in the scattering state. The percentage of light scattered in forward directions can be calculated from the measured scattered light intensity profile by using Eq. 3. The percentage of light blocked, namely the percentage of light that does not go through the windows, equal 100% subtracted by the percentage of light scattered in the forward direction. Note the light blocked is the sum of the light scattered in backward direction and the light reflected by the interfaces. Using the data shown in Figure 12, we calculate the percentage of light blocked by the windows and list the result in Table 1.

When the cell thickness is 10 μm, the percentages of light blocked of three types of windows are low, slightly higher than 10%. The capability to control energy flow is poor. However, when the cell thickness is 30 μm, the percentage of light blocked by the PDLC and PSCT windows are around 45%. The capability to control energy flow is not the best, but significant to reduce the heating effect of sunlight. The transmittance of the transparent state and the driving voltage, the voltage to obtain the maximum transmittance (for PDLC and PSCT windows), or the minimum transmittance (for PSLC window), are also listed in the table.

7 Conclusion

We studied the electro-optical properties of PDLC, PSLC, and PSCT switchable windows. We investigated how the factors such as monomer concentration, curing UV light intensity, helical pitch, and cell thickness affect their performance. In addition, we compared their capabilities to control the privacy and radiant energy flow. Regarding privacy control, we measured the transmittance of the windows with a collection angle of 4° and visually inspected images seen through them. All the windows, except the PDLC window with a thickness of 10 μm, can control privacy well. Regarding energy flow control, we measured the scattered light intensity as a function of the scattering angle in forward and backward directions, from which we calculated the percentage of light blocked. We observed that liquid crystals with small droplets (or domains), which can be achieved with high UV light intensity, high monomer concentration, and short pitch, scatter more light in directions with large scattering angles. When the cell thickness is 30 μm, PDLC and PSCT windows can block 45% incident light, which is satisfactory for energy flow control, and can be used for architectural and vehicle windows to control both privacy and radiant energy flow.

Data availability statement

The raw data supporting the conclusions of this article will be made available by the authors, without undue reservation.

Author contributions

All authors listed have made a substantial, direct, and intellectual contribution to the work and approved it for publication.

Conflict of interest

The authors declare that the research was conducted in the absence of any commercial or financial relationships that could be construed as a potential conflict of interest.

Publisher's note

All claims expressed in this article are solely those of the authors and do not necessarily represent those of their affiliated organizations, or those of the publisher, the editors and the reviewers. Any product that may be evaluated in this article, or claim that may be made by its manufacturer, is not guaranteed or endorsed by the publisher.

References

Bao, R., Liu, C. M., and Yang, D. K. (2009). Smart bistable polymer stabilized cholesteric texture light shutter. *Appl. Phys. Express* 2, 112401. doi:10.1143/apex.2.112401

Broer, D. J., Gossink, R. G., and Hikmet, R. A. M. (1990). Oriented polymer networks obtained by photopolymerization of liquid-crystalline monomers. *Angew. Makromol. Chem.* 183, 45–66. doi:10.1002/apmc.1990.051830103

Bronnikov, S., Kostromin, S., and Zuev, V. (2013). Polymer-dispersed liquid crystals: Progress in preparation, investigation, and application. *J. Macromol. Sci. Part B* 52, 1718–1735. doi:10.1080/00222348.2013.808926

Casini, M. (2015). Smart windows for energy efficiency of buildings. *Int. J. Civ. Struct. Engineering-IJCSE* 2, 273–281. doi:10.15224/978-1-63248-030-9-56

Castellón, E., and Levy, D. (2018). Smart windows based on liquid crystal dispersions. *Transparent Conduct. Mater.* 4, 337–365. doi:10.1002/9783527804603.ch5_4

Chel, A., and Kaushik, G. (2018). Renewable energy technologies for sustainable development of energy efficient building. *Alexandria Eng. J.* 57, 655–669. doi:10.1016/j.aej.2017.02.027

Coates, D. (1995). Polymer-dispersed liquid crystals. *J. Mat. Chem.* 5, 2063–2072. doi:10.1039/jm9950502063

Crawford, G. P., and Zumer, S. (1996). *Liquid crystals in complex geometries: Formed by polymer and porous*. London: Networks" CRC Press.

Dierking, I., Kosbar, L. L., Afzali-Ardakani, A., Lowe, A. C., and Held, G. A. (1998). Network morphology of polymer stabilized liquid crystals. *Appl. Phys. Lett.* 71, 2454–2456. doi:10.1063/1.120087

Dierking, I., Kosbar, L. L., Lowe, A. C., and Held, G. A. (1998). Polymer network structure and electro-optic performance of polymer stabilized cholesteric textures II. The effect of UV curing conditions. *Liq. Cryst.* 24 (3), 397–406. doi:10.1080/026782998207217

Drzaic, P. S. (1995). Droplet density, droplet size, and wavelength effects in PDLC light scattering. *Mol. Cryst. Liq. Cryst. Sci. Technol.* 261, 383–392. doi:10.1080/10587259508033483

Fuh, A. Y. G., Chih, S. Y., and Wu, S. T. (2017). Advanced electro-optical smart window based on PSLC using a photoconductive TiOPc electrode. *Liq. Cryst.* 45, 864–871. doi:10.1080/02678292.2017.1397214

Fung, Y. K., Yang, D. K., Ying, S., Chien, L. C., Zumer, S., and Doane, J. W. (2006). Polymer networks formed in liquid crystals. *Liq. Cryst.* 19, 797–801. doi:10.1080/02678299508031102

Halder, S., Shin, Y., Zhou, Z., Zhang, X., Hu, L., Yang, D.-K., et al. (2021). Aligned polymer dispersed liquid crystal film for light enhancement of quantum dot backlight. *Opt. Express* 29, 43241–43255. doi:10.1364/oe.446185

Hemaida, A., Ghosh, A., Sundaram, S., and Mallick, T. K. (2020). Evaluation of thermal performance for a smart switchable adaptive polymer dispersed liquid crystal (PDLC) glazing. *Sol. Energy* 195, 185–193. doi:10.1016/j.solener.2019.11.024

Higgins, D. A. (2000). Probing the mesoscopic chemical and physical properties of polymer-dispersed liquid crystals. *Adv. Mat.* 12 (4), 251–264. doi:10.1002/(sici)1521-4095(200002)12:4<251:aid-adma251>3.0.co;2-4

Huang, C. Y., Ke, S. W., and Chih, Y. S. (2006). Electro-optical performance of polymer stabilized cholesteric texture cell: The influence of chiral dopant and monomer concentration. *Opt. Commun.* 266, 198–202. doi:10.1016/j.optcom.2006.04.027

Hurley, S., Ma, J., and Yang, D.-K. (2009). P-108: A flexible display using dye-doped PSCT. *SID Symp. Dig.* 40, 1520–1523. doi:10.1889/1.3256602

Ji, S. M., Huh, J. W., Kim, J. H., Choi, Y., Yu, B. H., and Yoon, T. H. (2017). Fabrication of flexible light shutter using liquid crystals with polymer structure. *Liq. Cryst.* 44, 1429–1435. doi:10.1080/02678292.2017.1281452

Jiang, Y., Shin, Y., and Yang, D.-K. (2019). Dual-Mode switchable liquid-crystal window. *Phys. Rev. Appl.* 12, 054037. doi:10.1103/physrevapplied.12.054037

Ke, Y., Zhou, C., Zhou, Y., Wang, S., Chan, S. H., and Long, Y. (2018). Emerging thermal-responsive materials and integrated techniques targeting the energy-efficient smart window application. *Adv. Funct. Mat.* 28, 1800113. doi:10.1002/adfm.201800113

Kelly, J., Wu, W., and Palffy-muhoray, P. (2006). Wavelength dependence of scattering in PDLC films: Droplet size effects molecular crystals and liquid crystals science and technology. *Sect. A. Mol. Cryst. Liq. Cryst.* 223, 251–261. doi:10.1080/15421409208048256

Khandelwal, H., Loonen, R. C. G. M., Hensen, J. L. M., Debije, M. G., and Schenning, A. P. H. J. (2015). Electrically switchable polymer stabilised broadband infrared reflectors and their potential as smart windows for energy saving in buildings. *Sci. Rep.* 5, 11773–11779. doi:10.1038/srep11773

Klosowicz, S. J., and Zmija, J. (1995). Optics and electro-optics of polymer-dispersed liquid crystals: Physics, technology, and application. *Opt. Eng.* 34, 3440–3450. doi:10.1117/12.213241

Körner, B. S., Scheller, P. C., Beck, A., and Fricke, J. (1994). PDLC films for control of light transmission. *J. Phys. D. Appl. Phys.* 27, 2145–2151. doi:10.1088/0022-3727/27/10/023

Kumar, R., Raina, K. K., Kumar, R., and Raina, K. K. (2011). Polymer stabilized liquid crystals: Materials, physics and applications. *AIPC* 1393, 46–49.

Lackner, A., Margerum, J., Ramos, E., Lim M Lackner, K. A., Margerum, J. D., and Lim, K. (1989). Droplet size control in polymer dispersed liquid crystal films. *Liq. Cryst. Chem. Phys. Appl.* 1080, 53–61. doi:10.1117/12.976401

Lampert, C. M. (1998). Smart switchable glazing for solar energy and daylight control. *Sol. Energy Mater. Sol. Cells* 52, 207–221. doi:10.1016/s0927-0248(97)00279-1

Lee, K. M., Tondiglia, V. P., and White, T. J. (2015). Bistable switching of polymer stabilized cholesteric liquid crystals between transparent and scattering modes. *MRS Commun.* 5, 223–227. doi:10.1557/mrc.2015.40

Lee, W., and Kumar, S. (2021). *Unconventional liquid crystals and their applications*. Bristol, United Kingdom: IoP publishing ltd, 570.

Li, W., Cao, H., Kashima, M., Liu, F., Cheng, Z., Yang, Z., et al. (2008). Control of the microstructure of polymer network and effects of the microstructures on light scattering properties of UV-cured polymer-dispersed liquid crystal films. *J. Polym. Sci. B. Polym. Phys.* 46, 2090–2099. doi:10.1002/polb.21543

Li, W., Cao, Y., Cao, H., Kashima, M., Kong, L., and Yang, H. (2008). Effects of the structures of polymerizable monomers on the electro-optical properties of UV cured polymer dispersed liquid crystal films. *J. Polym. Sci. B. Polym. Phys.* 46, 1369–1375. doi:10.1002/polb.21471

Liang, H. H., Wu, C. C., Wang, P. H., and Lee, J. Y. (2011). Electro-thermal switchable bistable reverse mode polymer stabilized cholesteric texture light shutter. *Opt. Mat. (Amst).* 33, 1195–1202. doi:10.1016/j.optmat.2011.02.012

Lin, Y.-H., Chen, H.-S., Chiang, T.-H., Wu, C.-H., Hsu, H.-K., Kikuchi, H., et al. (2011). A reflective polarizer-free electro-optical switch using dye-doped polymer-stabilized blue phase liquid crystals. *Opt. Express* 19, 2556–2561. doi:10.1364/oe.19.002556

Long, L., and Ye, H. (2014). How to be smart and energy efficient: A general discussion on thermochromic windows. *Sci. Rep.* 4, 6427–6510. doi:10.1038/srep06427

Luckhurst, G., and Dunmur, D. (2017). *Liquid crystals*. London: Springer Handbooks.

Ma, R. Q., and Yang, D. K. (2000). Fréedericksz transition in polymer-stabilized nematic liquid crystals. *Phys. Rev. E* 61, 1567–1573. doi:10.1103/physreve.61.1567

Marinov, Y. G., Hadjichristov, G. B., and Petrov, A. G. (2009). Single-layered microscale linear-gradient PDLC material for electro-optics. *Cryst. Res. Technol.* 44, 870–878. doi:10.1002/crat.200900147

Nastal Ł, E., Uran´ska, ¸, Uran´ska, U., and Mucha, M. (1999). Effect of curing progress on the electrooptical and switching properties of PDLC system. *J. Appl. Polym. Sci.* 71, 455–463. doi:10.1002/(sici)1097-4628(19990118)71:3<455:aid-app12>3.0.co;2-7

Oh, M., Lee, C., Park, J., Lee, K., and Tae, S. (2019). Evaluation of energy and daylight performance of old office buildings in South Korea with curtain walls remodeled using polymer dispersed liquid crystal (PDLC) films. *Energies* 12, 3679. doi:10.3390/en12193679

Pascault, J. P., and Williams, R. J. J. (2009). *Epoxy polymers: New materials and innovations*. Hoboken, New Jersey, United States: John Wiley & Sons.

Paul Montgomery, G., Jr., West, J. L., and Tamura-Lis, W. (1998). Light scattering from polymer-dispersed liquid crystal films: Droplet size effects. *J. Appl. Phys.* 69, 1605. doi:10.1063/1.347256

Rajaram, C. v., Hudson, S. D., and Chien, L. C. (1996). Effect of polymerization temperature on the morphology and electrooptic properties of polymer-stabilized liquid crystals. *Chem. Mat.* 8, 2451–2460. doi:10.1021/cm9505207

Sanchez-Pena, J. M., Vazquez, C., Perez, I., Rodriguez, I., and Oton, J. M. (2002). Electro-optic system for online light transmission control of polymer-dispersed liquid crystal windows. *Opt. Eng.* 41, 1608–1611. doi:10.1117/1.1481049

Seo, Y.-W., Yoo, H.-S., Jin, Y., Lee, B.-Y., Lu, S., and Kwon, S.-B. (2014). Droplet size dependent electro-optical properties of PDLCs with one plastic substrate. *Mol. Cryst. Liq. Cryst.* 596, 97–105. doi:10.1080/15421406.2014.918329

Wong, K. v., and Chan, R. (2014). Smart glass and its potential in energy savings. *J. Energy Resour. Technol.* 136, 012002. doi:10.1115/1.4024768

Xu, C., Chu, Y. T., Hu, J. L., and Lu, H. B. (2016). Influence of helical twisting power on electro-optical properties of normal-mode polymer-stabilized cholesteric texture. *Liq. Cryst.* 31, 358–362. doi:10.3788/yjyxs20163104.0358

Yang, D. K., Cui, Y., Nemati, H., Zhou, X., and Moheghi, A. (2013). Modeling aligning effect of polymer network in polymer stabilized nematic liquid crystals. *J. Appl. Phys.* 114, 243515. doi:10.1063/1.4856295

Yang, D. K. (2012). Polymer stabilized cholesteric liquid crystal for switchable windows. *Liq. Cryst. Beyond Displays Chem. Phys. Appl.*, 2012, 505–523. doi:10.1002/9781118259993.ch16

Ying-Guey Fuh, A., Chen, C.-C., Liu, C.-K., Cheng, K.-T., Statman, D., Page, E., et al. (2009). Polarizer-free, electrically switchable and optically rewritable displays based on dye-doped polymer-dispersed liquid crystals. *Opt. Express* 17, 7088–7094. doi:10.1364/oe.17.007088

Yu, B. H., Ji, S. M., Kim, J. H., Huh, J. W., and Yoon, T. H. (2017). Fabrication of a dye-doped liquid crystal light shutter by thermal curing of polymer. *Opt. Mat. (Amst).* 69, 164–168. doi:10.1016/j.optmat.2017.04.029

Zhou, Y., You, Y., Liao, X., Liu, W., Zhou, L., Zhang, B., et al. (2020). Effect of polymer network topology on the electro-optical performance of polymer stabilized liquid crystal (PSLC) devices. *Macromol. Chem. Phys.* 221, 2000185. doi:10.1002/macp.202000185